Effect of realistic astrophysical inputs on the phase and shape of the weakly interacting massive particles annual modulation signal

Anne M. Green

Physics Department, Stockholm University, Stockholm, S106 91, Sweden

The orbit of the Earth about the Sun produces an annual modulation in the weakly interacting massive particles (WIMP) direct detection rate. If the local WIMP velocity distribution is isotropic then the modulation is roughly sinusoidal with maximum in June; however, if the velocity distribution is anisotropic the phase and shape of the signal can change. Motivated by conflicting claims about the effect of uncertainties in the local velocity distribution on the interpretation of the DAMA annual modulation signal (and the possibility that the form of the modulation could be used to probe the structure of the Milky Way halo), we study the dependence of the annual modulation on various astrophysical inputs. We first examine the approximations used for the Earth's motion about the Sun and the Sun's velocity with respect to the Galactic rest frame. We find that overly simplistic assumptions lead to errors of up to ten days in the phase and up to tens of percent in the shape of the signal, even if the velocity distribution is isotropic. Crucially, if the components of the Earth's velocity perpendicular to the motion of the Sun are neglected, then the change in the phase which occurs for anisotropic velocity distributions is missed. We then examine how the annual modulation signal varies for physically and observationally well-motivated velocity distributions. We find that the phase of the signal changes by up to 20 days and the mean value and amplitude change by up to tens of percent.

I. INTRODUCTION

Arguably the best motivated nonbaryonic dark matter candidate is the neutralino (the lightest supersymmetric particle), and direct detection experiments are just reaching the sensitivity required to probe the relevant region of parameter space [1]. Since the expected event rates are so small [$O(10^{-5}-10)$ counts kg^{-1}day^{-1} see, e.g., Refs. [2,3]] distinguishing a putative weakly interacting massive particle (WIMP) signal from backgrounds due to, for instance, neutrons from cosmic-ray-induced muons or natural radioactivity, is crucial. The Earth's motion about the Sun provides two potential WIMP smoking guns: (i) an annual modulation [4] and (ii) a strong direction dependence [5] of the event rate. In principle the dependence of the differential event rate on the atomic mass of the detector (see, e.g., Refs. [2,3]) is a third possibility; however, this would require good control of systematics for detectors composed of different materials. While direction sensitive detectors probably offer the best long-term prospects for the unambiguous detection of WIMPs, and development of such a detector is underway [6], annual-modulation searches are already feasible using large detector masses [7].

If the local WIMP velocity distribution is isotropic then the annual modulation is roughly sinusoidal with a maximum in early June (when the component of the Earth's velocity in the direction of the Sun's motion is largest) and amplitude of order a few percent. The DAMA Collaboration, using a detector consisting of NaI crystal scintillators, have detected an annual modulation with roughly these properties, which they interpret as a WIMP signal [7]. Assuming a standard halo model with a Maxwellian velocity distribution and circular velocity $v_c = 220$ km s^{-1}, they find a best fit WIMP mass

$m_\chi = 52$ GeV and cross section[1] $\zeta \sigma_p = 7.2 \times 10^{-9}$ nb with the 3-σ allowed region encompassing masses and cross sections in the range[2] 30 GeV$< m_\chi < 100$ GeV and 10^{-9} nb$< \zeta \sigma_p < 10^{-8}$ nb [7].

Taken at face value this allowed region is incompatible with the exclusion limits from the Cryogenic Dark Matter Search (CDMS) [9], Edelweiss [10], and Zeplin I [11] experiments. While these exclusion limits depend relatively weakly on the WIMP velocity distribution (varying by of order tens of percent for fixed v_c [12,13]) the annual modulation signal depends sensitively on the halo model assumed [14–21] and the region of WIMP mass–cross-section parameter space corresponding to the DAMA signal may be significantly enlarged if nonstandard halo models are considered [14,15,19]. In particular Belli *et al.* [19] carried out an extended analysis of the DAMA data, for a large range of halo models and parameters, and found a significant enlargement of the allowed region to encompasses masses in the range 30 GeV$< m_\chi < 270$ GeV and cross sections in the range 10^{-10} nb$< \zeta \sigma_p < 6 \times 10^{-8}$ nb. However, as recently pointed out by Copi and Krauss [20] and Fornengo and Scopel [21], the phase of the annual modulation can be significantly different if the WIMP velocity distribution is anisotropic and the time variation may not be close to sinusoidal [18,21]. In fact, in apparent contradiction to the results of Belli *et al.* [19], Copi and Krauss [20] found, considering a similar range of halo models, that the DAMA annual

---

[1]Here $\zeta = \rho_\chi / (0.3 \text{ GeV cm}^{-3})$ parametrizes the uncertainty in the local WIMP density, ρ_χ.

[2]The lower limit $m_\chi > 30$ GeV is imposed by hand and represents the somewhat model-dependent limit on the neutralino mass from accelerator sparticle searches (e.g., [8]).

modulation signal could not be made compatible with the exclusion limits from the CDMS and Edelweiss experiments.

Motivated by this apparent conflict, and also the possibility that if a WIMP annual modulation signal were detected its phase and shape [18,20,21] could allow us to probe the structure of the Milky Way (MW) halo, we study in detail the astrophysical uncertainties in the calculation of the annual modulation signal. In Sec. II we concentrate on the motion of the Earth relative to the Galactic rest frame. In Sec. III we discuss the local WIMP velocity distribution, in particular the importance of using physically and observationally reasonable models. In Sec. IV we examine the effects of the modeling of the Earth's motion and the local velocity distribution on the phase and amplitude of the signal and the extent to which it can be approximated by a sinusoidal variation, before concluding with a discussion in Sec. V.

II. MOTION OF THE EARTH

The differential WIMP elastic scattering rate due to scalar interactions is given by [2]

$$
\frac{dR}{dE}(E,t) = \zeta \sigma_p \left[\frac{\rho_{0.3}}{\sqrt{\pi} v_c} \frac{(m_p + m_\chi)^2}{m_p^2 m_\chi^3} A^2 T(E,t) F^2(q) \right], \quad (1)
$$

where $\rho_{0.3} = 0.3$ GeV cm^{-3} (and ζ is defined so that the local WIMP density is $\zeta \rho_{0.3}$), σ_p is the WIMP scattering cross section on the proton, v_c is the local circular velocity, A and $F(q)$ are the mass number and form factor of the target nuclei, respectively, E is the recoil energy of the detector nucleus, and $T(E)$ is defined, so as to be dimensionless, as [2]

$$
T(E,t) = \frac{\sqrt{\pi} v_c}{2} \int_{v_{min}}^{\infty} \frac{f_v(t)}{v} dv, \quad (2)
$$

where $f_v(t)$ is the WIMP speed distribution in the rest frame of the detector, normalized to unity, and v_{min} is the minimum WIMP speed that can cause a recoil of energy E:

$$
v_{min} = \left(\frac{E(m_\chi + m_A)^2}{2 m_\chi^2 m_A} \right)^{1/2}, \quad (3)
$$

where m_A is the atomic mass of the detector nuclei.

The WIMP velocity distribution in the rest frame of the detector is found by making a time-dependent Galilean transformation $\mathbf{v} \rightarrow \tilde{\mathbf{v}} = \mathbf{v} + \mathbf{v}_e(t)$, where $\mathbf{v}_e(t)$ is the Earth's velocity relative to the Galactic rest frame, which has two components: the Earth's orbit about the Sun and the Sun's motion with respect to the Galactic rest frame.

A. Orbit about the Sun

The Earth moves in a close to circular orbit, inclined at an angle of roughly 60° to the Galactic plane, with orbital speed

$v_e = 29.79$ km s^{-1}. The annual modulation is mainly determined by the component of the Earth's motion in the direction of the Sun's orbit:[3]

$$
v_{e,\odot}(t) = v_\odot + v_e \sin \gamma \cos \alpha(t), \quad (4)
$$

where $\alpha(t) = 2\pi(t - t_0)/T$, $T = 1$ yr, $t_0 \sim 153$ days (June 2nd), $\gamma \approx 30°$ is the angle between the axis of the ecliptic and the galactic plane, and t is measured in days. Since $v_\odot \gg v_e$, if the velocity distribution is close to isotropic, the differential event rate can be expanded in a Taylor series in $\cos \alpha(t)$ so that, to first order [4]:

$$
\frac{dR}{dE}(E,t) \approx R_0(E) + R_1(E)\cos \alpha(t), \quad (5)
$$

with $R_0(E) \gg R_1(E)$, i.e., the modulation is roughly sinusoidal.

A commonly used [16,22,15,20] expression for the Earth's motion in Galactic coordinates (X,Y,Z), where X is toward the Galactic center, Y in the direction of rotation, and Z toward the north Galactic pole, is

$$
\mathbf{v}_e(t) = v_e[-\sin \alpha(t), \cos \alpha(t) \sin \gamma, -\cos \alpha(t) \cos \gamma]. \quad (6)
$$

This expression assumes that the Earth's orbit is circular and the axis of the ecliptic lies in the Y-Z plane [16].

A more accurate expression for the components of the Earth's velocity relative to the Sun can be found by using the expression for the Sun's ecliptic longitude (from, e.g., p. 77 of Ref. [23]), $\lambda = L + 1°.915 \sin g + 0.020° \sin 2g$ where $L = 280°.460 + 0°.9856003t$ is the mean longitude of the Sun, corrected for aberration, $g = 357°.528 + 0°.9856003t$ is the mean anomaly (polar angle of orbit), and t is the time in days from 1200 Universal Time[4] on 31 Dec 1999, and transforming from ecliptic to Galactic coordinates (e.g., p. 13 of Ref. [23]). Lewin and Smith [3] carried out his procedure and found

$$
\mathbf{v}_e(t) = v_e(\lambda)[\cos \beta_x \sin(\lambda - \lambda_x), \cos \beta_y
$$
$$
\times \sin(\lambda - \lambda_y), \cos \beta_z \sin(\lambda - \lambda_z)], \quad (7)
$$

where $v_e(\lambda) = v_e[1 - e \sin(\lambda - \lambda_0)]$, $e = 0.016722$, and $\lambda_0 = 13° \pm 1°$ are the ellipticity of the Earth's orbit and the ecliptic longitude of the orbit's minor axis, respectively, and $\beta_i = (-5°.5303, 59°.575, 29°.812)$ and $\lambda_i = (266°.141, -13°.3485, 179°.3212)$ are the ecliptic latitudes and longitudes of the (X,Y,Z) axes, respectively.

Fornengo and Scopel [21] used a similar expression where the the nonuniform motion of the Sun in right ascension is neglected in the coordinate transformation so that the $\sin(\lambda - \lambda_i)$ terms in Eq. (7) above are replaced by $\cos[\omega(t - t_i)]$, where $t_i = (76.1, 156.3, 352.4)$ days and ω

---

[3]For simplicity we ignore the Sun's motion with respect to the local standard of rest in this section.

[4]Universal Time is equivalent to Greenwich Mean Time to within an accuracy of seconds.
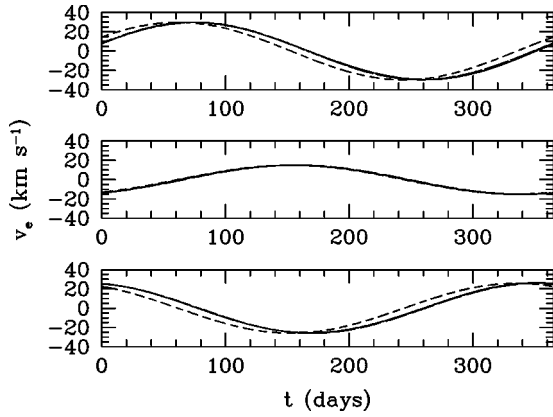
FIG. 1. The components of the orbital velocity of the Earth in Galactic X,Y,Z coordinates ($v_{e,X}$, top panel; $v_{e,Y}$, middle panel; and $v_{e,Z}$, bottom panel) found using the assumptions discussed in the text: (i) assuming that the Earth's orbit is circular and the ecliptic lies in the X-Y plane [Eq. (6), short dashed lines], (ii) ignoring the ellipticity of the Earth's orbit and the nonuniform motion of the Sun in right ascension [Eq. (8) and Ref. [18], long dashed line], (iii) including the ellipticity of the Earth's orbit but not the nonuniform motion of the Sun (Ref. [21], dot-dashed line), and (iv) including the ellipticity of the Earth's orbit and the nonuniform motion of the Sun [Eq. (7) and Ref. [3], solid line]. Time is measured in days from noon on 31 Dec 2002.

$=2\pi/(1$ year$)$. Gelmini and Gondolo [18] used a slightly simpler expression, which neglects the ellipticity of the Earth's orbit and the nonuniform motion of the Sun in right ascension. In terms of the Sun's ecliptic longitude, which under these approximations is given by $\tilde{\lambda}(t)=\omega(t-t_1)$, where t_1 is the spring (vernal) equinox, $t_1=79.55$ days,[5]

$$\mathbf{v}_e(t) = v_e[\hat{\mathbf{e}}_1 \sin \tilde{\lambda}(t) - \hat{\mathbf{e}}_2 \cos \tilde{\lambda}(t)], \qquad (8)$$

where $\hat{\mathbf{e}}_1$ and $\hat{\mathbf{e}}_1$ are in the Sun's direction at the spring equinox and summer solstice, respectively:

$$\hat{\mathbf{e}}_1 = (-0.0670, 0.4927, -0.8676),$$

$$\hat{\mathbf{e}}_2 = (-0.9931, -0.1170, 0.01032). \qquad (9)$$

These expressions for the components of the Earth's orbital velocity are displayed in Fig. 1, and the deviations between the expressions in Fig. 2. In the plots time is measured in days from noon on 31 Dec 2002, but the correct time (measured in days from noon on 31 Dec 1999) is used in the calculations. If time is erroneously measured from the beginning of the year rather than the beginning of 2000, then this leads to a horizontal shift in the curves of 0.27 days for every year elapsed since 2000. The deviations in the Y component are reassuring small (of order a few percent); however, assuming that the Earth's orbit is circular and the axis of the

---

[5]This figure is for 2003 and is accurate to within about 0.04 days. The time at which the spring equinox occurs increases by 0.24 days a year (see, e.g., Ref. [24]).
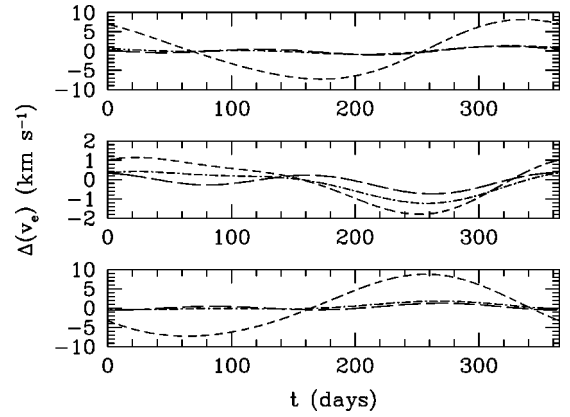

FIG. 2. The differences between the expressions for the velocity of the Earth in Galactic coordinates [$\Delta(v_{e,X}), \Delta(v_{e,Y}), \Delta(v_{e,Z})$, top, middle, and bottom panel, respectively] relative to the full expression, including the ellipticity of the Earth's orbit and the nonuniform motion of the Sun [Eq. (7) and Ref. [21]]. Line types as in Fig. 1. Note the larger scale used for $\Delta(v_{e,Y})$.

ecliptic lies in the Y-Z plane [Eq. (6)] leads to large errors in the X and Z components. The other three expressions are in relatively good agreement for all three components.

B. Motion of the Sun

We now consider the motion of the Sun, which can be divided into two components: the motion of the local standard of rest (LSR) and the Sun's peculiar motion with respect to the LSR, $v_{\odot,\mathrm{pec}}$. The "standard values" often used in WIMP event rate calculations date back to Kerr and Lynden-Bell's 1986 "Review of Galactic constants" [25]; however, since then the Hipparcos satellite has provided accurate measurements of the motions of large numbers of nearby stars, allowing more accurate determinations of the Galactic constants, so the "standard values" should be updated.

The standard value used for the Sun's peculiar motion, with respect to the LSR, is $v_{\odot,\mathrm{pec}}=(10,15,8)$ km s^{-1} [25], while Lewin and Smith [3] use $v_{\odot,\mathrm{pec}}=(9,12,7)$ km s^{-1}, with errors of order a few km s^{-1} in each component leading to an uncertainty of several days in the phase of the modulation [18]. The value determined more recently using data from Hipparcos is $v_{\odot,\mathrm{pec}}=(10.0,5.2,7.2)$ km s^{-1} [26,27], with the stated errors in each component being roughly 0.5 km s^{-1}.

Assuming that the MW is axisymmetric, then the motion of the LSR is, by definition, $(0,v_c(R_0),0)$, where $v_c(R_0)$ is the circular velocity at the solar radius. Kerr and Lynden-Bell combined a large number of independent determinations of the circular velocity and found $v_c=222.2$ km s^{-1}, with standard deviation 20 km s^{-1} [25]. The proper motions of Cepheids measured by Hipparcos allow accurate determinations of the Oort constants A and B [28], which lead to a value for the circular velocity, in terms of the Galactocentric distance R_0: $v_c(R_0)=(27.2\pm0.9)(R_0/\mathrm{kpc})$ km s^{-1} [27]. One possible caution is that this calculation assumes that stars move on circular orbits, which may lead to a systematic

error as the MW is not exactly axisymmetric [27]. Accurate very long baseline interferometry measurements of the proper motion of the SgrA* radio source at the Galactic center provides an alternative, marginally inconsistent, determination of v_c: $(30.1 \pm 0.9)(R_0/\text{kpc})$ km s^{-1} [29,27]. In this case nonzero peculiar motion of SgrA* produces a systematic error. Using $R_0 = 8.0 \pm 0.5$ kpc from the most recent compilation of determinations of R_0 [30] leads to $v_c(R_0) = (218 \pm 15)$ km s^{-1} from Cepheids and $v_c(R_0) = (241 \pm 17)$ km s^{-1} from SgrA*.

III. LOCAL WIMP VELOCITY DISTRIBUTION

Data analyses nearly always assume a standard halo model with an isotropic Maxwellian velocity distribution:

$$f(\mathbf{v}) = \frac{1}{\pi^{3/2} v_{c,h}^3} \exp(-\mathbf{v}^2/v_{c,h}^2), \tag{10}$$

where $v_{c,h}$ is the contribution of the halo to the local circular velocity, which corresponds to a spherically symmetric density distribution with $\rho \propto r^{-2}$, i.e., an isothermal sphere. Observations and numerical simulations indicate that galaxy halos are in fact triaxial and anisotropic, however (see Ref. [13] for a review). As the size [14,16–21] and phase [20,21] of the annual modulation signal depend quite sensitively on the halo model assumed, the realistic modeling of the WIMP velocity distribution is crucial when extracting parameters or exclusion limits from data or comparing results from different experiments.

The steady state phase-space distribution function of a collection of collisionless particles is given by the collisionless Boltzmann equation, and the velocity dispersions, $\langle v_i^2 \rangle$, of the system are calculated via the Jeans equations, which are found by taking moments of the collisionless Boltzmann equation (see, e.g., [31]). Solutions to the Jean's equations have the property that the tensor $\sigma_{ij}^2 \equiv \overline{(v_i - \bar{v}_i)(v_j - \bar{v}_j)}$ is symmetric, so that at any point a set of orthogonal axes can be chosen such that $\boldsymbol{\sigma}$ is diagonal (i.e., $\sigma_{ij}^2 = \sigma_{ii}^2 \delta_{ij}$) [31]. However, as discussed in Refs. [31,32], there is no equation of state relating the components of the velocity dispersion to the density, so solving the Jeans equations requires assumptions, which may or may not be physically reasonable, about the shape and/or orientation of $\boldsymbol{\sigma}$. Evans *et al.* [32] presented the logarithmic ellipsoidal model [which has potential $\Phi(x,y,z) = (v_c^2/2)\ln(x^2 + y^2 p^{-2} + z^2 q^{-2})$] which is the simplest triaxial, scale-free generalization of the isothermal sphere. They argued that principle axes aligned with conical coordinates correspond to physical distribution functions and calculated the corresponding velocity dispersions. On the axes of the halo conical coordinates are locally equivalent to cylindrical polar coordinates and the local velocity distribution can be approximated by a multivariate Gaussian with principle axes aligned with the (X,Y,Z) Galactic axes. This form has been widely used in calculations of the WIMP direction detection rate [32,22,19,13,20,21]; however, a multivariate Gaussian with arbitrary velocity dispersions need not correspond to a physically sensible halo model. For instance
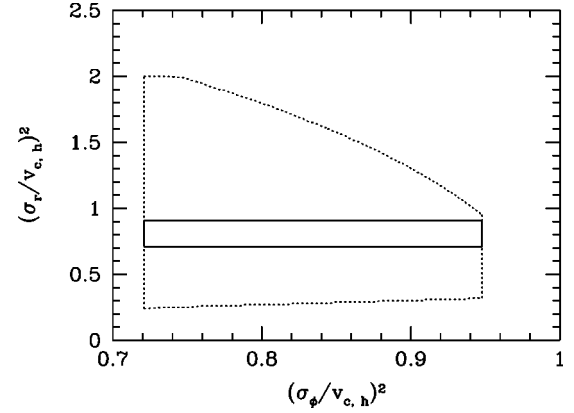

FIG. 3. Physically and observationally reasonable values of σ_r and σ_ϕ [$\sigma_z = (v_{c,h}^2 - \sigma_\phi^2)^{1/2}$]. Inside the dotted lines the ratio of any two of the velocity dispersions is no greater than 1:3 and inside the solid lines the anisotropy parameter β is in the range $0 < \beta < 0.4$. Restricting the axial ratios of the density distribution would further rule out some sets of values inside the solid lines.

Evans *et al.* do not consider parameter values for which the ratio of any two of the velocity dispersions is more than 3:1, so as to avoid models which are afflicted by instabilities [32].

We will now briefly examine what sets of values of the velocity dispersions are reasonable for the logarithmic ellipsoidal model, if the Sun is located on the intermediate axis of the halo (the deviations from an isotropic velocity distribution are smaller on the major axis [32,13]). On the intermediate axis the velocity distribution can be written as

$$f(\mathbf{v}) = \frac{1}{(2\pi)^{3/2} \sigma_r \sigma_\phi \sigma_z} \exp\left(-\frac{v_r^2}{2\sigma_r^2} - \frac{v_\phi^2}{2\sigma_\phi^2} - \frac{v_z^2}{2\sigma_z^2} \right), \tag{11}$$

with the velocity dispersions given by

$$\sigma_r^2 = \frac{v_{c,h}^2 p^{-4}}{(2+\gamma)(1 - p^{-2} + q^{-2})},$$

$$\sigma_\phi^2 = \frac{v_{c,h}^2 (2q^{-2} - p^{-2})}{2(1 - p^{-2} + q^{-2})},$$

$$\sigma_z^2 = \frac{v_{c,h}^2 (2 - p^{-2})}{2(1 - p^{-2} + q^{-2})}, \tag{12}$$

where p and q are constants which satisfy $0 \le q \le p \le 1$ and are related to the axial ratios of the density distribution, $I_{1,2}$, by

$$I_1^2 = \frac{p^2(p^2 q^2 + p^2 - q^2)}{q^2 + p^2 - p^2 q^2},$$

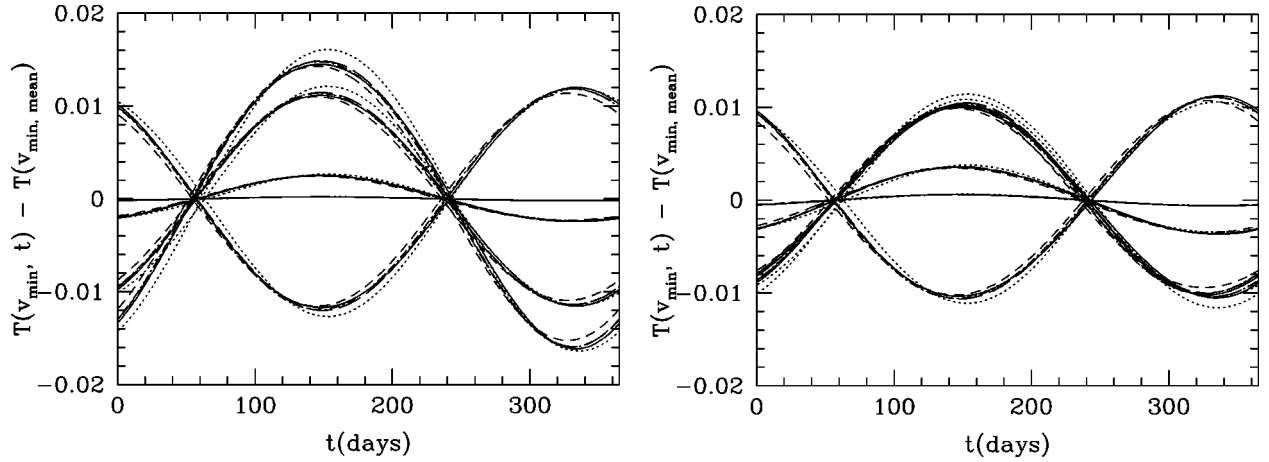$$I_2^2 = \frac{q^2(p^2 q^2 - p^2 + q^2)}{q^2 + p^2 - p^2 q^2}, \tag{13}$$

FIG. 4. The dependence of $T(v_{min}, t)$ on the approximations used when calculating the Earth's orbit for, from top to bottom at $t=0$, $v_{min}=100, 500, 400, 300$, and 200 km s^{-1} with line types as in Fig. 1 for the standard halo model (upper panel) and for the fiducial triaxial model, see the text for details (bottom panel). Note the change in the phase of the annual modulation for $v_{min}=100$ km s^{-1} (see the text and Ref. [41] for a further discussion of the change in phase which occurs for small v_{min}). We have fixed $v_{c,h}=150$ km s^{-1} and $v_{\odot,pec} = (10.0, 5.2, 7.2)$ km s^{-1} here.

and γ is a constant isotropy parameter, which in the spherical limit $p=q=1$ is related to the anisotropy parameter

$$\beta = 1 - \frac{\langle v_\theta^2 \rangle + \langle v_\phi^2 \rangle}{2 \langle v_r^2 \rangle}, \qquad (14)$$

by $-\gamma=2\beta$. Note that $\sigma_\phi^2 + \sigma_z^2 = v_{c,h}^2$ and $\sigma_\phi > \sigma_z$.

If we require $\sigma_j/3 < \sigma_i < 3\sigma_j$, so as to avoid models which might be affected by instabilities [32], then the velocity dispersions lie in the ranges $0.32 < \sigma_z/v_{c,h} < 0.71$, $0.71 < \sigma_\phi/v_{c,h} < 0.95$, and $0.24 < \sigma_r/v_{c,h} < 2.0$. If we also require that $0 < \beta < 0.4$, as found at the solar radius in simulated halos [33], then σ_r is further restricted to $0.71 < \sigma_r/v_{c,h} < 0.92$. In Fig. 3 we plot the values of σ_r and σ_ϕ ($\sigma_z^2 = v_{c,h}^2 - \sigma_\phi^2$) which satisfy these two requirements. We still need to check that the axial ratios of the density distribution are in reasonable agreement with observed and simulated

galaxy halos. There is no simple algebraic relation between the I_i's and the σ_i's. If we require $0.6 < I_1 < 1.0$ and $0.3 < I_2 < 1.0$ (see, e.g., Ref. [34] for a review of constraints on the shape of dark matter halos) then some of the previously allowed sets of velocity dispersions are now excluded.

The logarithmic ellipsoidal model may not be a unique solution to the Jeans equations (and there is no reason to expect the Sun to be located on one of the axes of the halo), but otherwise there is no reason for the principle axes of the velocity distribution to correspond to the axes of the halo. In other words a multivariate Gaussian velocity distribution with axes corresponding to the axes of the halo and arbitrary velocity dispersions may not correspond to a physically reasonable halo model. While the constraints on the axial ratios and anisotropy of the halo we have imposed are not cast in stone, they illustrate that only restricted sets of values of the velocity dispersions correspond to observationally and physically reasonable halo models, and that the ratios of the ve-
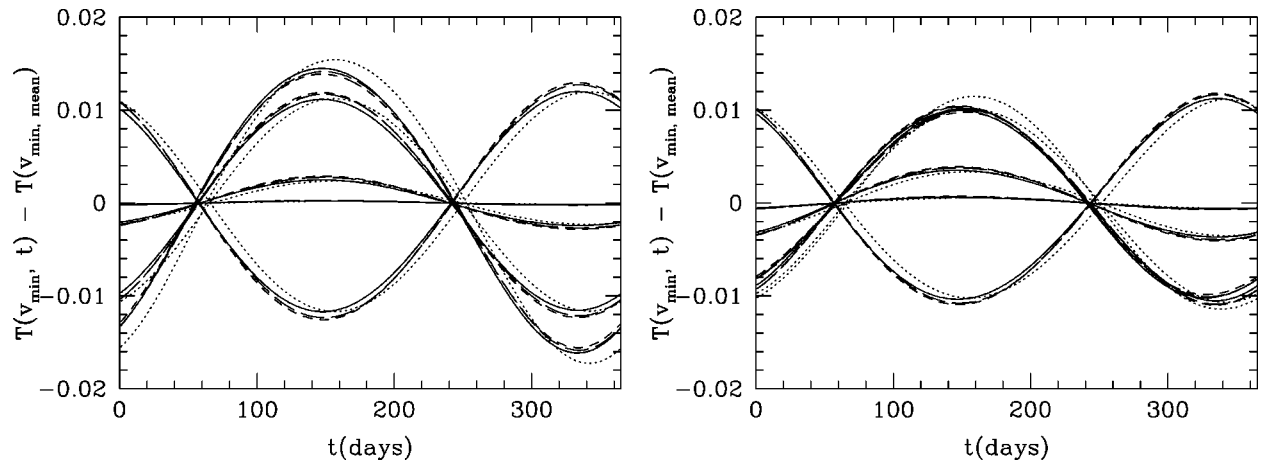

FIG. 5. As Fig. 4 for the dependence of $T(v_{min}, t)$ on the values used for the Sun's velocity with respect to the LSR ($v_{\odot,pec}$, in km s^{-1}): (10.0, 5.2, 7.2) (Refs. [26,27], solid line), (0, 0, 0) (dotted line), (10, 15, 8) (Ref. [25], short dashed line), (9, 12, 7) (Ref. [3], long dashed line). The full expression for the Earth's orbit [Ref. [3] and Eq. (7)] is used here.

TABLE I. The time, t_p, at which $T(v_{\min}, t)$ is largest; the largest percentage deviation from $T(v_{\min}, t)$ calculated using the full expression for the Earth's velocity, $\Delta^{\mathrm{LS}}_{\max}$; the largest percentage deviation from a sinusoidally varying $T(v_{\min}, t)$ with the same mean, amplitude, and t_p, $\Delta^{\sin}_{\max}$ for each of the expressions for the Earth's velocity discussed in Sec. II for the standard isotropic halo model. Using only the component of the Earth's motion in the Galactic plane is denoted by "zeroth order"; "first order" denotes the assumption that the axis of the ecliptic lies in the Y-Z plane [Eq. (6)]; "GG" denotes neglecting the ellipticity of the Earth's orbit and the nonuniform motion of the Sun [Ref. [18] and Eq. (8)]; "FS" denotes neglecting the nonuniform motion of the Sun (Ref. [21]); and "LS" includes the ellipticity of the Earth's orbit and the nonuniform motion of the Sun [Ref. [3] and Eq. (7)]. Where a range of values is given the quantity varies with $v_{\min}$ and the left (right) hand value is for $v_{\min} = 200$ (500) km s^{-1}. Here we have fixed $v_{\mathrm{c,h}} = 150$ km s^{-1} and used $v_{\odot,\mathrm{pec}} = (10.0, 5.2, 7.2)$ km s^{-1}.

Earth's orbit	t_{peak} (days)	$\Delta^{\mathrm{LS}}_{\max}$	$\Delta^{\sin}_{\max}$
Zeroth order	153	$-2.4\% - -15.6\%$	$0.1\% - -11.1\%$
First order	145	$2.6\% - 19.0\%$	$0.3\% - -6.6\%$
GG	148–149	$2.2\% - 15.6\%$	$0.4\% - -7.2\%$
FS	146–147	$2.2\% - 15.8\%$	$0.5\% - -6.7\%$
LS	147–148	n/a	$0.7\% - -5.1\%$

locity dispersions cannot be too large. Simulations provide further support for this argument. Helmi, White, and Springel [35] examined the simulation particles within a 4 kpc box located 8 kpc from the center of a Milky Way like halo and found that, apart from a clump of fast moving particles from a late accreting subhalo, the velocity distribution was well approximated by a multivariate Gaussian, with principal axis velocity dispersions in the ratio 1:1.08:1.27. If, in fact, the local dark matter distribution is not smooth (see below for discussion of this possibility), then the local velocity distribution could not be approximated by a multivariate Gaussian with any set of velocity dispersions. We conclude that the large velocity dispersion ratios found by Fornengo and Scopel to produce extreme distortions of the annual modulation [(1:5:4) and (10:1:3)] [21] are unlikely to correspond to a realistic halo model.

It is possible that the local WIMP distribution may not be completely smooth, or in other words that the phase-space distribution has not reached a steady state. The density and velocity distributions of the "particles" in numerically simulated halos are relatively smooth at the solar radius [33,35]; however, WIMP direct detection experiments probe the dark matter distribution within a local sub-mpc region and even the highest resolution simulations have less than 100 "particles" per kpc^3. Furthermore the first neutralino clumps to form have mass more than ten orders of magnitude smaller than the smallest subhalos resolved in numerical simulations [36], and it is possible that the cores of some of these first

small, high density, clumps could survive to the present day [36,13,37]. Stiff and Widrow [38] have recently developed a technique which uses test particles to probe the velocity distribution at a single point within a numerical simulation. They find a local velocity distribution consisting of a series of discrete peaks, and argue that the smooth background found previously in simulations may be, at least partly, a consequence of the use of a finite volume to measure the velocity distribution. Even if the local phase-space distribution bears no trace of the first WIMP clumps to form, more massive subhalos which have been accreted onto the MW relatively recently, and have sufficiently eccentric orbits, could produce coherent streams of high velocity WIMPs at the solar radius [39,35].

An additional complication is that the contribution of the visible components of the MW to the circular velocity at the Solar radius is non-negligible, and may even dominate that of the halo (see, e.g., Refs. [40,33]). Self-consistent halo models can, in principle, be built (taking into account various observations) using Eddington's formula [17,19]; however, building mass models of the Milky Way is a complex and ill-constrained process [40,27]; a small change in the observational constraints can lead to a large change in the properties of the dark halo. In Dehnen and Binney's mass models, where the halo is described by a spheroidal density distribution, the contribution of the MW halo to the circular velocity at the solar radius lies in the range $v_{\mathrm{c,h}}(R_0) = 110 - 180$ km s^{-1} [40], while Moore *et al.* find, for halos with a

TABLE II. As in Table I for the fiducial triaxial halo model.

Earth's orbit	t_p (days)	$\Delta^{\mathrm{LS}}_{\max}$	$\Delta^{\sin}_{\max}$
Zeroth order	153	$-1.5\% - -11.6\%$	$0.1\% - -4.7\%$
First order	147–142	$2.2\% - 12.5\%$	$0.3\% - -1.0\%$
GG	153–146	$2.0\% - 9.6\%$	$0.4\% - -2.3\%$
FS	151–144	$2.0\% - 9.9\%$	$0.4\% - -2.7\%$
LS	152–144	n/a	$0.3\% - -3.2\%$

TABLE III. As in Table I for the motion of the Sun relative to the LSR, with Δ_{max}^H the maximum deviation from $T(v_{min})$ found using $v_{\odot,pec} = (10.0, 5.2, 7.2)$ km s^{-1}, as found from Hipparcos data [26]. The full expression for the Earth's orbit [Ref. [3] and Eq. (7)] is used here.

$v_{\odot,pec}$(km s^{-1})	t_p (days)	Δ_{max}^H	Δ_{max}^{sin}
(0, 0, 0)	157	3.1% – 19.3%	0.7% – 5.6%
(10, 15, 8)	148	4.0% – 30.0%	0.6% – 4.9%
(9, 12, 7)	149	2.7% – 20.0%	0.6% – 4.9%
(10.0, 5.2, 7.2)	147–148	n/a	0.7% – 5.1%

central density cusp $\rho \propto r^{-1.5}$, taking 190 km s$^{-1} < v_c(R_0) < 230$ km s^{-1} and using a smaller set of constraints, 100 km s$^{-1} < v_{c,h}(R_0) < 120$ km s^{-1} [33]. We therefore conclude that a relatively conservative range of values is 100 km s$^{-1} < v_{c,h}(R_0) < 200$ km s^{-1}, and that the "standard" value, $v_{c,h}(R_0) = 220$ km s^{-1}, is probably too large.

IV. RESULTS

To compare theoretical predictions with experimental data requires the detector atomic mass, form factor and resolution, and the relationship between the nuclear recoil energy and the energy detected, to be taken into account (see, e.g., Ref. [3]). As the DAMA Collaboration's raw data is not publicly available instead of working with the differential event rate we look at the detector independent quantity $T(v_{min}, t)$, as defined in Eq. (2). The relation between v_{min} and the detected energy is given, for various target nuclei and WIMP masses, in Fig. 4 of Ref. [21]. For reference, the DAMA experiment has a measured energy threshold of 2 keV which corresponds (for iodine which dominates) to a recoil energy threshold of 22 keV, which for $m_\chi = 50(200)$ GeV requires a minimum WIMP velocity $v_{min} = 309(146)$ km s^{-1}.

A. Motion of the Earth

We will start by examining the effects of the modeling of the motion of the Earth on the phase and shape of the annual modulation signal. We use two fiducial halo models: the standard halo model (with an isotropic Maxwellian velocity distribution) and the logarithmic ellipsoidal model [32], with the Earth located on the intermediate axis and parameter values $p = 0.9, q = 0.8$, and $\gamma = -0.62$ corresponding to axial ratios $1:0.78:0.48$ and $\beta = 0.4$. The later model is intended as a specific, somewhat arbitrary but not unreasonable, example of an anisotropic halo model. In both cases we take $v_{c,h} = 150$ km s^{-1}. In Fig. 4 we plot[6] $T(v_{min}, t)$ produced by each of the expressions for the Earth's motion discussed in Sec. II, for five specific values of v_{min}. As has long been known (see e.g. Ref. [41]), for small v_{min} the phase of the modulation is reversed. Furthermore, as v_{min} is increased the

TABLE IV. As Table III for the fiducial triaxial halo model.

$v_{\odot,pec}$(km s^{-1})	t_p (days)	Δ_{max}^{hyp}	$\Delta_{max}^{sinsoid}$
(0, 0, 0)	159–153	2.4% – 13.8%	0.1% – 2.6%
(10, 15, 8)	152–146	2.8% – 20.1%	0.2% – 2.5%
(9, 12, 7)	153–147	1.9% – 13.6%	0.2% – 2.8%
(10.0, 5.2, 7.2)	152–143	n/a	0.3% – 3.2%

amplitude of the modulation reaches a maximum before decreasing again. For the standard halo model this maximum occurs at roughly 220 km s^{-1}, whereas for the fiducial triaxial model the maximum is at around 250 km s^{-1} and $T(200$ km s$^{-1}, t) \sim T(300$ km s$^{-1}, t)$. In Fig. 5 we plot $T(v_{min}, t)$ produced by each of the sets of values for the Sun's motion with respect to the LSR discussed in Sec. II.

To provide a quantitative comparison Tables I and II contain the day at which $T(v_{min}, t)$ (and hence the differential event rate) is largest, t_p, the maximum deviation from $T(v_{min}, t)$ calculated using the full expression for the Earth's motion [Eq. (7)], and the maximum deviation from a sinusoidally varying $T(v_{min}, t)$ with the same mean, amplitude, and t_p, for the standard halo model and the fiducial triaxial model, respectively. Tables III and IV contain the same data for $T(v_{min}, t)$ found using each of the sets of values for the Sun's velocity with respect to the LSR. For reference the DAMA Collaboration have carried out a fit to the modulation of their data using the function $A \cos[2\pi(t - t_p)/T]$, and when T is fixed at one year they found $t_p = 144 \pm 13$ days [7].

The time at which the event rate is maximum[7] varies by up to ten days, depending on the expression used for the Earth's velocity, and depends on v_{min} if the velocity distribution is anisotropic [20,21]. If only the component of the Earth's velocity in the Y direction is used, then the change in the phase which occurs for anisotropic halos is missed. The three sophisticated expressions produce results which are in reasonably good agreement, however, with maximum deviations of around a few percent for $v_{min} \lesssim 400$ km s^{-1}. For larger v_{min} the exact form of the high energy tail of the speed distribution becomes important, so that using a different expression for the Earth's velocity produces a large fractional change in $T(v_{min}, t)$. As the mean event rate is small for large v_{min}, the absolute errors are small, though, and therefore not so important from an experimental point of view.

The maximum deviations from a sinusoidal $T(v_{min}, t)$ are no more than a few percent for $v_{min} \lesssim 400$ km s^{-1}, as is expected since the error in neglecting the second and higher order terms in the Taylor expansion is $\mathcal{O}((v_{e,Y}/v_\odot)^2) \sim 0.01$). The amplitude of the annual modulation is largest for large v_{min} [4], as in the tail of the speed distribution the fraction of particles with speed greater than some fixed value changes significantly with $v_e(t)$, the Taylor expansion is then inappropriate and the deviation from sinusoidal variation becomes large (up to around 10%). For the fiducial anisotropic model we have chosen the deviations happen to be smaller

---

[6]Our plots look superficially different to those of Fornengo and Scopel as they normalize to the event rate on 1 January whereas we subtract the mean event rate.

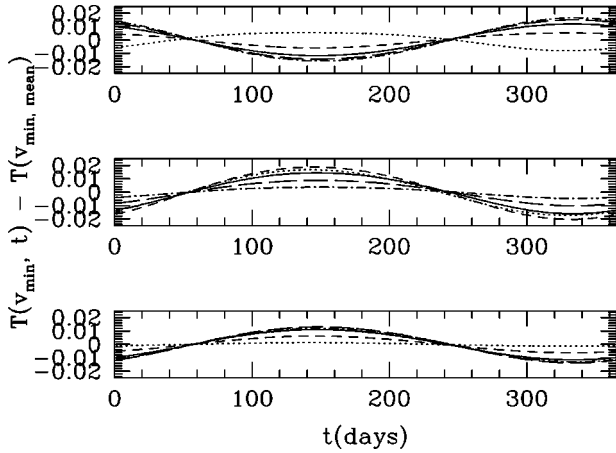[7]For simplicity we neglect the "flip" in the phase which occurs at small v_{min} in this discussion.

FIG. 6. The dependence of $T(v_{min},t)$ on the contribution of the halo to the local circular velocity, $v_{c,h}$ for the standard halo model for (from top to bottom) $v_{min}=100,200$ and 300 km s^{-1} and $v_{c,h}=100$ (dotted line), 125 (short dashed line), 150 (solid line), 175 (long dashed line), and 200 km s^{-1} (dot-dashed line).

FIG. 7. The shift in the phase, $\Delta(t_p)$, and the fractional change in the amplitude of $T(v_{min},t)$, $\Delta(amp)$ (relative to the standard isotropic halo model) for the logarithmic ellipsoidal model with the Sun located on the intermediate axis for parameter values for which the ratio of any two of the velocity dispersions is no greater than 1:3 (dots) and for which also the anisotropy parameter is in the range $0<\beta<0.4$ and the axes ratios are $0.6<I_1<1$ and $0.3<I_2<1$ (crosses). From top to bottom $v_{min}=100,300,500$ km s^{-1}. The contribution of the halo to the local circular velocity is fixed at $v_{c,h}=150$ km s^{-1}.

than for the standard isotropic halo model, but this is not the case in general.

The time at which the event rate is maximum is relatively weakly dependent on the Sun's velocity with respect to the LSR (provided that it is not neglected entirely); however, the maximum deviation from $T(v_{min},t)$ found using the Hipparcos values for the Sun's velocity depends strongly on the component in the Y direction and can be large. Finally we note that combining a poor approximation for the Earth's orbit with an erroneous value for the Sun's velocity with respect to the LSR would produce even larger errors.

B. Local WIMP velocity distribution

The region of WIMP mass-cross-section parameter space consistent with the DAMA annual modulation signal depends strongly on the contribution of the halo to the circular velocity at the solar radius, $v_{c,h}(R_0)$ [14]. To explicitly illustrate the reason for this, in Fig. 6 we plot $T(v_{min},t)$ for $v_{min}=100,200$, and 300 km s^{-1} for values of $v_{c,h}$ in the range 100–200 km s^{-1}, for the standard halo model. As $v_{c,h}$ (and hence the typical WIMP velocity) is decreased the value of v_{min}, at which the modulation flips phase and also that at which the amplitude of the modulation reaches a local maximum are both smaller. For instance, for $v_{c,h}=100$ km s^{-1} the local maximum occurs at roughly $v_{min}=155$ km s^{-1} compared with $v_{min}=220$ km s^{-1} for $v_{c,h}=150$ km s^{-1}.

As our aim is to examine how physical and observational constraints restrict changes in the phase and shape of the annual modulation signal (rather than to carry out a detailed comparison with experimental data) we focus on the logarithmic ellipsoidal model, which reproduces some of the important features (triaxiality and velocity anisotropy) of real galaxy halos. We examine the form of $T(v_{min},t)$, with the Sun located on the intermediate axis, for the sets of values of the velocity dispersions that are unlikely to lead to instabilities and those which also correspond to halos with axis ratios and velocity anisotropy consistent with observed and simu-
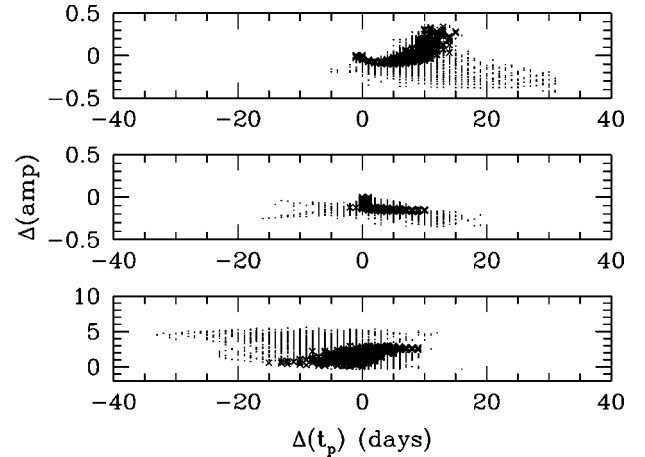
lated halos, as discussed in Sec. III. In Fig. 7 we plot the shift in the time at which $T(v_{min},t)$ is maximum, Δt_p, and the fractional change in the amplitude of the variation of $T(v_{min},t)$ relative to that for the standard isotropic halo model, for $v_{min}=100,300$, and 500 km s^{-1}, fixing $v_{c,h}=150$ km s^{-1}. In Fig. 8 we plot the fractional changes in the mean and amplitude of the variation of $T(v_{min},t)$ relative to the standard isotropic halo model.

If we consider all sets of velocity dispersions for which $\sigma_j/3<\sigma_i<3\sigma_j$, the shift in t_p has magnitude of up to 40 days and is quite strongly dependent on v_{min}. The change in the amplitude is of order 10 s of percent for $v_{min}=100$ and 300 km s^{-1} and up to a factor of 5 for $v_{min}=500$ km s^{-1},
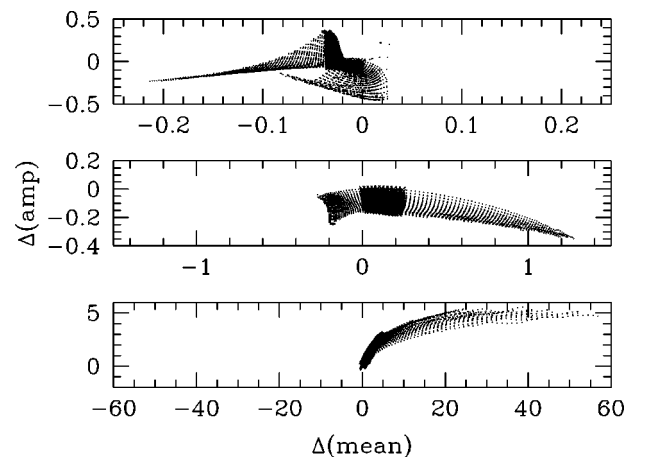

FIG. 8. As Fig. 7 for the fractional change in the mean, $\Delta(mean)$, and amplitude, $\Delta(amp)$, of $T(v_{min},t)$ (relative to the standard isotropic halo model).
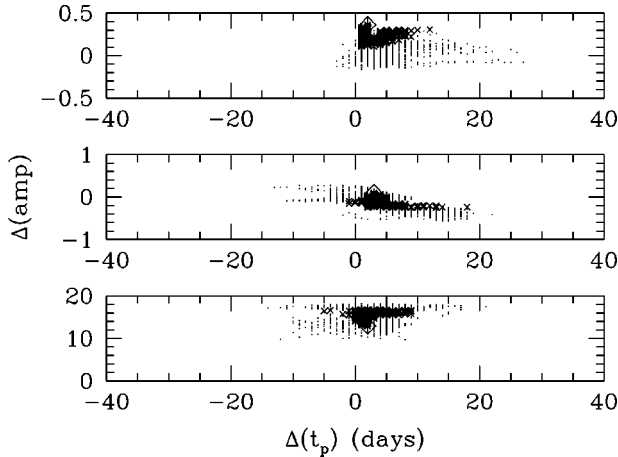
FIG. 9. As in Fig. 7 for the logarithmic ellipsoidal model with $v_{c,h}=200$ km s^{-1}, compared to the standard isotropic halo with $v_{c,h}=150$ km s^{-1}. The diamonds denote the standard isotropic halo with $v_{c,h}=200$ km s^{-1}.

while the change in the mean is even larger increasing from 10 s of percent for $v_{min}=100$ km s^{-1} to more than an order of magnitude at $v_{min}=500$ km s^{-1}. The large change in the mean and amplitude for large v_{min} occur because the logarithmic ellipsoidal model has a more extended tail of high velocity particles than the standard halo model [13,32]; however, as noted in Sec. III, the mean event rate is very small for large v_{min}. When only sets of velocity dispersions which correspond to halos with realistic axis ratios and velocity anisotropy are considered the maximum shift in t_p is roughly 50% smaller and the the maximum change in the mean signal is roughly an order of magnitude smaller, which illustrates the importance of only considering velocity distributions that are physically and/or observationally reasonable. Note that the standard isotropic halo model (which has $\beta=0$ and $I_1=I_2=1$) lies at the edge of the observational constraints we impose.
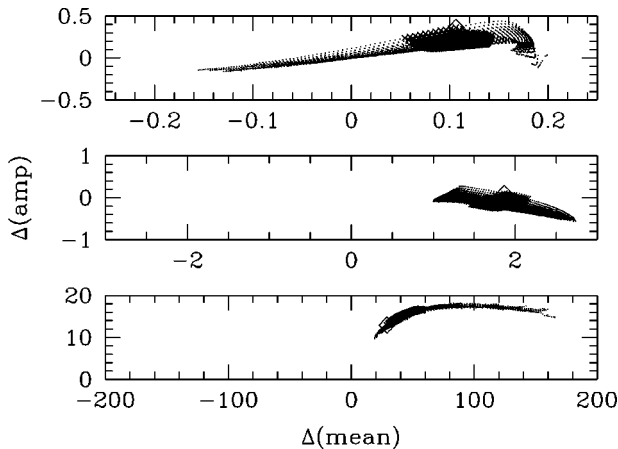
In Figs. 9 and 10 we plot the shifts in the mean, ampli-

FIG. 10. As in Fig. 8 for the logarithmic ellipsoidal model with $v_{c,h}=200$ km s^{-1}, compared to the standard isotropic halo with $v_{c,h}=150$ km s^{-1}. The diamonds denote the standard isotropic halo with $v_{c,h}=200$ km s^{-1}.

tude, and phase relative to the standard isotropic halo model with $v_{c,h}=150$ km s^{-1}, for the same sets of velocity dispersion ratios but now with $v_{c,h}=200$ km s^{-1}. The changes in the signal due to the change in $v_{c,h}$ are of the same order of magnitude as the changes from varying the other parameters of the model.

We do not find shifts in t_p as large as those found by Copi and Krauss [20] and Fornengo and Scopel [21]. For many of the sets of parameter values we have considered the shift in t_p is large enough to be incompatible with the phase of the DAMA annual modulation signal, however. This suggests that if all three components of the Earth's velocity are included when calculating the event rate, then the consideration of anisotropic halo models may not lead to as large an increase in the region of WIMP mass and cross-section parameter space corresponding to the DAMA annual modulation signal as found in Ref. [19]. As the DAMA data are not publicly available, however, it is not possible to confirm this.

Finally we overview the effect of streams of particles on the annual modulation signal. A stream of particles with negligible velocity dispersion would produce a contribution to $T(v_{min},t)$ which is a step,[8] the position and amplitude of which varies with time [39]:

$$T_s(v_{min},t)=\begin{cases} \dfrac{\sqrt{\pi}v_{c,h}}{2}\dfrac{\rho_s}{\zeta\rho_{0.3}}\dfrac{1}{v_s(t)} & \text{for } v_{min}<v_s(t),\\[2ex] 0 & \text{for } v_{min}>v_s(t), \end{cases}$$

(15)

where ρ_s is the density of the stream and $v_s(t)$ is the speed of the stream in the rest frame of the detector, which is time dependent due to the time dependence of the Earth's velocity. The variation of the amplitude and position of the step depend on the relative orientation of the Earth's orbit and the orbit of the clump; for a clump of fixed velocity the closer the alignment of the clump's path with the Earth's orbit the larger the variation in $v_s(t)$ (in the extremely improbable case that the clump's path was perpendicular to the Earth's orbit there would be no variation). As outlined in Ref. [39], if such a step were detected in the differential energy spectrum then the density, speed, and direction of the stream responsible could, in principle (with a large number of events and a detector with good energy resolution), be recovered. Multiple streams would produce multiple steps at different energies with different temporal variations, which might be difficult to disentangle. Even if most of the dark matter is smoothly distributed a high velocity ($v_s \gtrsim 500$ km s^{-1}) stream of particles from a late accreting clump could produce a step in the differential event rate at large energy, the position of which would be modulated as discussed above [39]. However, as the event rate decreases roughly exponentially with increasing energy this would only be detectable with very large statistics (large target mass and exposure). A similar signal would be produced if there is a population of extragalactic WIMPs [42].

---

[8]The velocity dispersion would in fact be finite, but small, and would lead to a broadening in the step [39].

V. DISCUSSION

We have investigated the effect of uncertainties in astrophysical inputs (the motion of the Earth with respect to the Galactic rest frame and the local WIMP velocity distribution) on the calculation of the WIMP annual modulation signal. Accurate calculation of the shape and phase of the annual modulation signal requires all three components of the Earth's velocity with respect to the Sun to be taken into account properly. If the components perpendicular to the Sun's motion are neglected, the (energy dependent) shift in t_p, which occurs if the local velocity distribution is anisotropic, is missed. Neglecting the motion of the Sun with respect to the local standard of rest, $v_{\odot,\mathrm{pec}}$, leads to an error of around 10 days in t_p, and uncertainties in $v_{\odot,\mathrm{pec}}$ lead to an error of order a few days in t_p (as stated in Ref. [18]) and errors in the shape of the signal which grow from a few percent at low energies to more than 10% at high energy. Approximating the modulation with a sinusoid with the same mean, amplitude, and phase produces errors of up to 10%. The errors in t_p are crucial when comparing theoretical expectations with the modulation observed by the DAMA Collaboration [7] (which has phase $t_p = 144 \pm 13$ days). The errors in the shape of the signal induced by uncertainties in the Earth's motion are currently less important, but may become important for annual modulation searches with tonne size detectors (such as the planned GENIUS detector [43]), especially if we want to extract information about the local velocity distribution from an observed signal.

If the local WIMP velocity is anisotropic then the phase [20,21], amplitude [15,16,18], and even shape [18,21] of the annual modulation signal can change. We have investigated, focusing on the logarithmic ellipsoidal halo model, how the form of the annual modulation changes for parameter choices which correspond to physically and observationally reasonable halo models. We found that for reasonable sets of values for the velocity dispersions the shift in t_p, which is energy dependent, can be up to 20 days and the mean and amplitude of the signal change by tens of percent, at experimentally accessible energies. It is possible that other halo models could produce larger changes in the annual modulation signal; however, we have shown, in the context of this model, that restricting the choice of parameter values to those that are physically and observationally reasonable seriously restricts the changes in the signal. We have also argued that a multivariate Gaussian velocity distribution, with axes corresponding to the axes of the halo and velocity dispersions with large ratios, is unlikely to correspond to a physically reasonable halo model.

It is often assumed that the contribution of the luminous components of the MW to the circular velocity at the solar radius is negligible so that $v_{c,h}(R_\odot) \sim v_c(R_\odot) \approx 220 \ \mathrm{km \ s^{-1}}$. This is not the case and in fact there is a large uncertainty in the value of $v_{c,h}(R_\odot)$ [40,33], which is important since (as we saw in Sec. III B) the mean and amplitude of the event rate (and hence the region of WIMP mass- cross-section parameters space corresponding to an observed modulation [14,19]) depend quite sensitively on $v_{c,h}(R_\odot)$.

Finally we discussed the possibility that the local WIMP distribution is not completely smooth [33,39,38]. If the local dark matter distribution consists of a number of streams of particles with small velocity dispersion, then the event rate would contain a number of steps, the amplitude and position of which would vary with time [38]. Even if there is a smooth background WIMP distribution, high velocity streams from late accreting subhalos [39,35] may be detectable with good energy resolution and a large number of events.

In summary, it is important to properly take into account astrophysical uncertainties (not just in the WIMP velocity distribution, but also in the motion of the detector with respect to the Galactic rest frame) when calculating the WIMP annual modulation signal. Analyzing data assuming a sinusoidal modulation with fixed phase could lead to erroneous constraints on or best fit values for the WIMP mass or cross section, or even worse a WIMP signal could be overlooked. On the other hand, using unrealistic halo models or parameter values could lead to overly restrictive exclusion limits or a misleadingly large range of allowed values of the WIMP mass and cross section.

ACKNOWLEDGMENT

[1] L. Bergström, Rep. Prog. Phys. **63**, 793 (2000).

[2] G. Jungman, M. Kamionkowski, and K. Griest, Phys. Rep. **267**, 195 (1996).

[3] J.D. Lewin and P.F. Smith, Astropart. Phys. **6**, 87 (1996).

[4] A.K. Drukier, K. Freese, and D.N. Spergel, Phys. Rev. D **33**, 3495 (1986); K. Freese, J. Frieman, and A. Gould, *ibid.* **37**, 3388 (1988).

[5] D.N. Spergel, Phys. Rev. D **37**, 1353 (1988).

[6] D.P. Snowden-Ifft, C.J. Martoff, and J.M. Burwell, Phys. Rev. D **61**, 101301(R) (2000).

[7] R. Bernabei *et al.*, Phys. Lett. B **389**, 757 (1996); **408**, 439 (1997); **424**, 195 (1998); **450**, 448 (1999); **480**, 23 (2000).

[8] R. Barate *et al.*, Phys. Lett. B **499**, 67 (2001).

[9] R. Abusaidi *et al.*, Phys. Rev. Lett. **84**, 5699 (2000); D.

Abrams *et al.*, Phys. Rev. D **66**, 122003 (2002).

[10] A. Benoit *et al.*, Phys. Lett. B **545**, 43 (2002).

[11] N.J. Smith *et al.*, to appear in the Proceedings of 4th International Workshop on Identification of Dark Matter, York, 2002, see also http://www.shef.ac.uk/~phys/idm2002/talks/

[12] M. Kamionkowski and A. Kinkhabwala, Phys. Rev. D **57**, 3256 (1998); F. Donato, N. Fornengo, and S. Scopel, Astropart. Phys. **9**, 247 (1998).

[13] A.M. Green, Phys. Rev. D **66**, 083003 (2002).

[14] M. Brhlik and L. Roszkowski, Phys. Lett. B **464**, 303 (1999); P. Belli *et al.*, Phys. Rev. D **61**, 023512 (2000).

[15] A.M. Green, Phys. Rev. D **63**, 043005 (2001).

[16] J.D. Vergados, Phys. Rev. Lett. **83**, 3597 (1999); Phys. Rev. D **62**, 023519 (2000); **63**, 063511 (2001); A.M. Green, *ibid.* **63**,

103003 (2001); J.D. Vergados and D. Owen, Astrophys. J. **589**, 17 (2003); J. D. Vergados, Phys. Rev. D **67**, 103003 (2003).

[17] P. Ullio and M. Kamionkowski, J. High Energy Phys. **03**, 049 (2001).

[18] G. Gelmini and P. Gondolo, Phys. Rev. D **64**, 023504 (2001).

[19] P. Belli, R. Cerulli, N. Forengo, and S. Scopel, Phys. Rev. D **66**, 043503 (2002).

[20] C.J. Copi and L.M. Krauss, Phys. Rev. D **67**, 103507 (2003).

[21] N. Fornengo and S. Scopel, astro-ph/0301132.

[22] C.J. Copi and L.M. Krauss, Phys. Rev. D **63**, 043507 (2001).

[23] K. R. Lang, *Astrophysical Formulae* (Springer-Verlag, New York, 1999).

[24] *Planetary and Lunar Coordinates 2001–2020* (The Stationery Office, Norwich, UK, 2000); relevant data available courtesy of the U.S. Naval Observatory, Astronomical Applications Department at http://aa.usno.navy.mil/data/docs/EarthSeasons.html

[25] F.J. Kerr and D. Lynden-Bell, Mon. Not. R. Astron. Soc. **221**, 1023 (1986).

[26] W. Dehnen and J.J. Binney, Mon. Not. R. Astron. Soc. **298**, 387 (1998).

[27] J.J. Binney and M. Merrifield, *Galactic Astronomy* (Princeton University Press, Princeton, NJ, 1998).

[28] M. Feast and P. Whitelock, Mon. Not. R. Astron. Soc. **291**, 683 (1997).

[29] D.C. Baker, *Unsolved Problems of the Milky Way*, IAU Symposium No. 169, edited by D. Blitz and P. Teuben (Dordrecht, Kluwer, 1996), p. 198.

[30] M.J. Reid, Annu. Rev. Astron. Astrophys. **31**, 345 (1998).

[31] J.J. Binney and S. Tremaine, *Galactic Dynamics* (Princeton University Press, Princeton, NJ, 1987).

[32] N.W. Evans, C.M. Carollo, and P.T. de Zeeuw, Mon. Not. R. Astron. Soc. **318**, 1131 (2000).

[33] B. Moore *et al.*, Phys. Rev. D **64**, 063508 (2001).

[34] P.D. Sackett, *Galaxy Dynamics*, ASP Conf. Series No. 182, edited by D. Merritt, J.A. Sellwood, and M. Valluri (ASP, San Francisco, 1999), p. 393.

[35] A. Helmi, S.D.M. White, and V. Springel, Phys. Rev. D **66**, 063502 (2002).

[36] S. Hofmann, D.J. Schwarz, and H. Stöcker, Phys. Rev. D **64**, 083507 (2001).

[37] V. Berenzinsky, V. Dokuchaev, and Y. Eroshenko, astro-ph/0301551.

[38] D. Stiff and L.M. Widrow, Phys. Rev. Lett. **90**, 211301 (2003).

[39] D. Stiff, L.M. Widrow, and J. Frieman, Phys. Rev. D **64**, 083516 (2001).

[40] W. Dehnen and J.J. Binney, Mon. Not. R. Astron. Soc. **294**, 429 (1998).

[41] K. Griest, Phys. Rev. D **37**, 2703 (1988); J.R. Primack, D. Seckel, and B. Sadoulet, Annu. Rev. Nucl. Sci. **38**, 751 (1988); F. Hasenbalg, Astropart Phys. **9**, 339 (1998).

[42] K. Freese, P. Gondolo, and L. Stodolsky, Phys. Rev. D **64**, 123502 (2001).

[43] H.V. Klapdor-Kleingrothaus, Nucl. Phys. B (Proc. Suppl.) **110**, 58 (2002).